NASA TN D-116

NASA TN D-116

TECHNICAL NOTE

D-116

AERODYNAMIC DAMPING AT MACH NUMBERS OF 1.3 AND 1.6 OF A CONTROL SURFACE ON A TWO-DIMENSIONAL WING BY THE FREE-OSCILLATION METHOD

By W. J. Tuovila and Robert W. Hess

Langley Research Center
Langley Field, Va.

NATIONAL AERONAUTICS AND SPACE ADMINISTRATION

WASHINGTON February 1960

NATIONAL AERONAUTICS AND SPACE ADMINISTRATION

TECHNICAL NOTE D-116

AERODYNAMIC DAMPING AT MACH NUMBERS OF 1.3 AND 1.6 OF A CONTROL SURFACE ON A TWO-DIMENSIONAL WING BY THE FREE-OSCILLATION METHOD[1]

By W. J. Tuovila and Robert W. Hess

L
8
1
6

SUMMARY

Tests have been made at two supersonic speeds to obtain experimentally the aerodynamic damping characteristics of a control surface on a two-dimensional wing. The control surface had a chord of 1.67 inches (1/3 of the wing chord) and a span of 7.25 inches and was supplied in three materials (steel, aluminum, and magnesium) having different mass, inertia, and stiffness properties. Two wing sections were tested, one being a 65A004 section and the other a 5-percent-thick hexagonal section. The test results are compared with results calculated by two- and three-dimensional oscillating air-force theories. At a Mach number of 1.6, both theories are in fairly good agreement with the experimental results. At a Mach number of 1.3, both theories predict negative (unstable) damping, whereas the tests indicate that the damping is slightly positive (stable). The in-phase or aerodynamic stiffness coefficients predicted by both theories are slightly higher than the experimentally determined coefficients.

INTRODUCTION

Theoretical studies have indicated that at low supersonic speeds control surfaces with a single degree of torsional freedom can encounter unstable aerodynamic damping at some values of reduced frequencies. Since existing theories do not account for many flow effects which may influence the problem, tests were made to obtain some experimentally determined aerodynamic damping coefficients for comparison with theoretical values. Aerodynamic in-phase or stiffness coefficients and out-of-phase or damping coefficients were determined for a 1/3-chord control surface attached to a two-dimensional wing at zero angle of attack. Wings with hexagonal and 65A004 section shapes were used. The tests were made at Mach numbers of 1.3 and 1.6 over a reduced-frequency range from 0.029 to 0.074. This paper presents the test results and compares them with results calculated using two- and three-dimensional theories for

---

[1]Supersedes declassified NACA Research Memorandum L56A26a by W. J. Tuovila and Robert W. Hess, 1956.

oscillating air forces. The test results are also compared with the results of some damping tests made on a control surface attached to a triangular wing (ref. 1).

SYMBOLS

b_a	semichord of control surface, ft
δ	control-surface deflection, radians
f_o	natural frequency of rotation of control surface about hinge line at zero airspeed, cps
f_t	natural frequency of rotation of control surface about hinge line at test Mach number, cps
g_o	damping coefficient associated with f_o
g_t	damping coefficient associated with f_t
l_a	span of control surface, ft
m_a	mass of control surface, slugs/ft of span
$\bar{N}_5$	in-phase aerodynamic coefficient per foot of span
$\bar{N}_6$	out-of-phase or damping coefficient per foot of span
M	Mach number
V	airspeed, fps
ρ	air density, slugs/cu ft
$\omega_o = 2\pi f_o$	
$\omega_t = 2\pi f_t$	
k	reduced frequency, $b_a \omega_t / V$
k_t	reduced frequency at test Mach number
k_a	spring constant, ft-lb/radian

L 8 1 6

C_h hinge-moment coefficient

$C_{h_{\dot{\delta}}} = -2K\overline{N}_6$

I_a mass moment of inertia about control hinge line, slug-ft^2/ft of span

$$r_a^2 = \frac{I_a}{m_a b_a^2}$$

L
8
1
6

$$\mu = \frac{m_a}{4\rho b_a^2}$$

Dots over symbols denote derivatives with respect to time.

MODELS AND TEST METHODS

Wing, control-surface, and hinge details are given in figure 1. Control surfaces made of steel, aluminum, and magnesium were tested on two steel wing models which differed only in section. One wing model had a 65A004 section and the other had a 5-percent-thick hexagonal section. Each wing had a 5-inch chord and spanned the tunnel test section with one end clamped in the sidewall and the other end pinned in the sidewall. The control-surface chord was 1/3 of the wing chord. Steel hinges of various stiffnesses were used to attach the control surfaces to the wings at three points. There was a gap of about 0.02 inch between the wing and the control surface. Table 1 lists some of the physical parameters of the models. The masses and inertias were determined experimentally and include the contribution of the hinges.

The tests were made at Mach numbers of 1.3 and 1.6 (ρ = 0.00090 slug/cu ft, V = 1,430 fps and ρ = 0.00066 slug/cu ft, V = 1,760 fps, respectively) in the 9- by 18-inch Langley supersonic flutter apparatus, which is an intermittent-flow blow-down tunnel operated at atmospheric stagnation pressure. The testing technique used was first to obtain "no-wind" damping decrements with the wing in the testing configuration by flicking the control surface. The control surface was then deflected, the tunnel was brought up to speed, and the control surface was released and a "wind-on" damping decrement was obtained. The air flow was then stopped and the process was repeated using hinges of different stiffness.

The initial amplitude of both the "no-wind" and the "wind-on" oscillations was not controlled precisely. It was judged by eye to range from about $\pm 1^{\circ}$ to $\pm 2\frac{1}{2}^{\circ}$, the larger amplitudes occurring at the lowest frequencies.

The system for deflecting the control is illustrated in figure 1 and consisted of a wire with an eye on the end which was inserted through a small hole at the trailing edge of the control surface. A straight release wire was then inserted through the eye of the cocking wire. The control surface was cocked by pulling the cocking wire until the desired deflection was obtained. The control surface was released by pulling the release wire out of the eye of the cocking wire.

L
8
1
6

Damping decrements were obtained from a strain gage glued to a thin metal strip fastened to the wing and control surface. This metal strip followed the control-surface motion and the strain-gage output was amplified and fed into a recording oscillograph.

REDUCTION OF DATA

The experimental decay decrements were reduced to average total supersonic aerodynamic coefficients $\bar{N}_5$ and $\bar{N}_6$ as was done in reference 2 for subsonic flow. All damping terms are assumed proportional to amplitude and in phase with velocity. The following equation of equilibrium,

$$I_a\ddot{\delta} + k_a\left(1 + ig_o\right)\delta = -4\rho b_a{}^2V^2k^2\delta\left(\bar{N}_5 + i\bar{N}_6\right) \tag{1}$$

leads to the following results for the in-phase component,

$$\bar{N}_5 = \mu r_a{}^2\left[1 - \left(\frac{\omega_o}{\omega_t}\right)^2\right] \tag{2}$$

and for the out-of-phase or damping component,

$$\bar{N}_6 = \mu r_a{}^2\left[g_t - g_o\left(\frac{\omega_o}{\omega_t}\right)^2\right] \tag{3}$$

The details of the analysis are given in the appendix.

It may be noted that the damping component is not obtained from just the difference in the damping coefficients of the "wind-on" and "no-wind" decrements. Instead, the "no-wind" damping coefficient is reduced by the factor $(\omega_o/\omega_t)^2$, which accounts for the difference in the structural damping coefficient due to the difference in frequency between "wind-off" and "wind-on" conditions. It is of interest to note that at $M = 1.3$ the "no-wind" damping coefficient g_o was usually larger than the "wind-on" damping coefficient g_t but the factor $(\omega_o/\omega_t)^2$ made the aerodynamic damping coefficient $\bar{N}_6$ slightly positive.

L-816

The experimentally determined $\bar{N}_5$ and $\bar{N}_6$ are compared with two- and three-dimensional air-force coefficients obtained from references 3 and 4. For comparison with the results obtained in reference 1, the damping coefficient $\bar{N}_6$ is expressed in stability notation using viscous-type damping terms as follows:

$$C_{h_{\dot{\delta}}} = \frac{\partial C_h}{\partial \frac{b\dot{\delta}}{V}} = -2k\bar{N}_6 \tag{4}$$

RESULTS AND DISCUSSION

Presentation of Data and Comparison With Theory

The control surfaces were attached to two-dimensional wings set at zero angle of attack. The aerodynamic in-phase and damping coefficients were obtained from the decay records and frequencies obtained in both still air and at the test Mach numbers of 1.3 and 1.6 and the data are presented in table 2. Sample "wind-off" and "wind-on" decrements are shown in figures 2(a) and 2(b). The hinge axis was so near the leading edge of the control surface that it was assumed to be there. The aerodynamic damping coefficients $\bar{N}_6$ are presented in figure 3 and the in-phase coefficients $\bar{N}_5$ are presented in figure 4. The aerodynamic coefficients are plotted against the reduced frequency, based on the control-surface semichord.

The experimental results are compared with the two-dimensional theory of reference 3 by assuming the control surface to be a wing oscillating about its leading edge and with the three-dimensional theory of reference 4, assuming a sealed gap between the wing and the control surface. The theoretical results are also plotted on figures 3 and 4. Both theories predict negative aerodynamic damping at $M = 1.3$; however, the three-dimensional theory predicts only about 1/2 the damping of the two-dimensional theory. The experimental aerodynamic damping at $M = 1.3$ is slightly positive and both theories approach it as k increases. At $M = 1.6$ both theories are in good agreement with the experimental damping results, the three-dimensional theory giving slightly higher values than the two-dimensional theory.

The experimental in-phase aerodynamic coefficients $\bar{N}_5$ presented in figure 4 are fairly consistent and both theories predict the trends well. The two-dimensional theory gives slightly higher values than the three-dimensional theory does and both theories yield values that are higher than the experimental.

It appears that linearized flow theory, when applied to flow around trailing-edge control surfaces, begins to break down at low Mach numbers in the neighborhood of 1.3 or less. Adding an aspect-ratio correction to the two-dimensional-flow theory improves the results; however, some basic differences between the actual and the idealized flow appears to affect the results. Wing thickness, boundary layer, and the gap between the wing and control surface are some factors whose effects are not included in the theory. Also, the experimental results were obtained from decaying oscillations, whereas the theory assumes constant-amplitude oscillations. At $M = 1.6$ the theory seems to compensate for these effects and the agreement is good.

Comparison With Control-Surface Data for a Triangular Wing

The results of the present tests are compared in figure 5 with those of reference 1 through the Mach number range. Results for an amplitude of $\pm 3^{\circ}$ at a maximum k value of 0.03 from reference 4 are compared with the results of the present tests for amplitudes of about $\pm 2^{\circ}$ at k values of 0.045. The damping coefficients are expressed in stability notation as $C_{h_{\dot{\delta}}}$. The difference in the present results and those of reference 1 may be the result of differences in flow caused by the wings. It may be noted that in reference 1 the control surface is attached to an aspect-ratio-2 triangular wing and not to a two-dimensional wing. In reference 1 the damping varied from a small degree of instability at $M = 1.3$ to neutral stability at $M = 1.9$, whereas the present tests indicate slight stability at $M = 1.3$ and considerable stability at $M = 1.6$. The two- and three-dimensional theory results are also presented in figure 5.

GENERAL OBSERVATIONS

At $M = 1.3$ there is considerable scatter in the results but the damping coefficients in all but one case are positive. This scatter is due to the sensitivity of the equation for $\overline{N}_6$ to small changes in measured damping between the "wind-off" and "wind-on" conditions when the aerodynamic damping is low. No flutter was observed during these tests which indicates that the total damping was positive and shows that the aerodynamic damping could have been, at most, only slightly negative since the structural damping was small. At $M = 1.6$, where the aerodynamic damping is higher, the scatter is considerably reduced. Any effects due to wing-profile or control-surface material is lost within the scatter of the results.

The structural damping g_o was principally in the range 0.006 to 0.01 with a few extreme values of $g_o = 0.004$ on the low end and $g_o = 0.034$ on the high end. This spread in the structural damping coefficient is believed to be due to variations in the hinge clamping force. Also, the structural damping coefficient generally decreased with decrease in amplitude and some unusually large changes are noted in table 2(a) for $\mu r_a^2 = 650$. The damping coefficients recorded in table 2(a) were measured near the maximum amplitude of oscillation.

The aerodynamic damping may also be affected by amplitude; however, since the present tests were made without amplitude control, no such effect can be determined. No appreciable amplitude effect is indicated in reference 1 at Mach numbers from 1.3 to 1.9 while reference 5 shows considerable effect for amplitudes up to $\pm 5^\circ$ at Mach numbers near 1.0.

Wing bending motion may also affect the results by introducing a translation degree of freedom to the control surface. Although the wing motion was not measured, it is believed to have been very slight since the wing was clamped at one end and pinned at the other. As the control-surface frequency approached the wing resonant frequency, the wing amplitude would increase rapidly and any bending effect should become evident. At $M = 1.6$ the NACA 65A004 wing with control surface $\mu r_a^2 = 378$ reached the wing resonant frequency at $k = 0.069$ and yielded essentially the same results as the hexagonal wing with control surface $\mu r_a^2 = 427$ where the control-surface frequency was 85 percent of the wing resonant frequency. The NACA 65A004 wing would have had about 5 times the amplitude of the hexagonal wing at this k value which indicates that the wing bending amplitude had no apparent effect on the damping results.

CONCLUDING REMARKS

The results of the tests of a control surface attached to a two-dimensional wing at zero angle of attack indicate that at a Mach number of 1.3, a slight amount of aerodynamic damping exists on the control surface, whereas both two- and three-dimensional theories predict negative damping. At a Mach number of 1.6 the control surface has considerable aerodynamic damping which both two- and three-dimensional theories predict quite well. Both theories predict the trends of the in-phase aerodynamic coefficients, but they yield results which are slightly higher than experimental values. These results were obtained at reduced frequencies from 0.029 to 0.074.

Langley Research Center,
National Aeronautics and Space Administration,
Langley Field, Va., January 9, 1956.

APPENDIX

DERIVATION OF AERODYNAMIC COEFFICIENTS $\overline{N}_5$ AND $\overline{N}_6$

The supersonic aerodynamic coefficients $\overline{N}_5$ and $\overline{N}_6$ are derived from the following equations of equilibrium, where the damping is assumed proportional to the displacement and in phase with the velocity:

For "wind-on" condition (aerodynamic and structural),

$$I_a\ddot{\delta} + k_t\left(1 + ig_t\right)\delta = 0 \tag{A1}$$

and for "no-wind" condition (structural only),

$$I_a\ddot{\delta} + k_a\left(1 + ig_o\right)\delta = 0 \tag{A2}$$

where

$$\pi g = \text{Logarithmic decrement}$$

Then,

$$k_t\delta - k_a\delta = \text{Aerodynamic spring force} \tag{A3}$$

and

$$k_t g_t\delta - k_a g_o\delta = \text{Aerodynamic damping force} \tag{A4}$$

Equation (A4) implies that the structural damping force is independent of frequency.

By definition

$$\overline{N}_5 = \frac{\text{Aerodynamic spring force}}{4\rho {b_a}^2 V^2 k^2 \delta}$$

$$= \frac{\left(k_t - k_a\right)\delta}{4\rho {b_a}^2 V^2 k^2 \delta} \tag{A5}$$

and

$$\overline{N}_6 = \frac{\text{Aerodynamic damping force}}{4\rho {b_a}^2 V^2 k^2 \delta}$$

$$= \frac{\left(k_t g_t - k_a g_o\right)\delta}{4\rho {b_a}^2 V^2 k^2 \delta} \tag{A6}$$

For small values of damping

$$\omega_t^2 = k_t \big/ I_a \qquad \omega_o^2 = k_a \big/ I_a \tag{A7}$$

and by definition reduced frequency is

$$k = b_a \omega_t \big/ V \tag{A8}$$

Substituting equations (A7) and (A8) into (A5) and (A6) gives L816

$$\overline{N}_5 = \frac{I_a\left(\omega_t^2 - \omega_o^2\right)}{4\rho b_a^2 V^2 \dfrac{b_a^2 \omega_t^2}{V^2}} = \frac{I_a}{4\rho b_a^4}\left[1 - \left(\frac{\omega_o}{\omega_t}\right)^2\right] \tag{A9}$$

and

$$\overline{N}_6 = \frac{I_a\left(\omega_t^2 g_t - \omega_o^2 g_o\right)}{4\rho b_a^2 V^2 \dfrac{b_a^2 \omega_t^2}{V^2}} = \frac{I_a}{4\rho b_a^4}\left[g_t - g_o\left(\frac{\omega_o}{\omega_t}\right)^2\right] \tag{A10}$$

Finally, substituting

$$\mu r_a^2 = \frac{m_a}{4\rho b_a^2} \frac{I_a}{m_a b_a^2} = \frac{I_a}{4\rho b_a^4}$$

into equations (A9) and (A10) results in

$$\overline{N}_5 = \mu r_a^2\left[1 - \left(\frac{\omega_o}{\omega_t}\right)^2\right] \tag{A11}$$

and

$$\overline{N}_6 = \mu r_a^2\left[g_t - g_o\left(\frac{\omega_o}{\omega_t}\right)^2\right] \tag{A12}$$

REFERENCES

1. Reese, David E., Jr.: An Experimental Investigation at Subsonic and Supersonic Speeds of the Torsional Damping Characteristics of a Constant-Chord Control Surface of an Aspect Ratio 2 Triangular Wing. NACA RM A53D27, 1953.

2. Widmayer, Edward, Jr., Clevenson, Sherman A., and Leadbetter, Sumner A.: Some Measurements of Aerodynamic Forces and Moments at Subsonic Speeds on a Rectangular Wing of Aspect Ratio 2 Oscillating About the Midchord. NACA TN 4240, 1958. (Supersedes NACA RM L53F19.)

3. Garrick, I. E., and Rubinow, S. I.: Flutter and Oscillating Air-Force Calculations for an Airfoil in a Two-Dimensional Supersonic Flow. NACA Rep. 846, 1946. (Supersedes NACA TN 1158.)

4. Berman, Julian H.: Lift and Moment Coefficients for an Oscillating Rectangular Wing-Aileron Configuration in Supersonic Flow. NACA TN 3644, 1956.

5. Martin, Dennis J., Thompson, Robert F., and Martz, C. William: Exploratory Investigation of the Moments on Oscillating Control Surfaces at Transonic Speeds. NACA RM L55E31b, 1955.

L
8
1
6

TABLE 1.- SOME CONTROL-SURFACE PHYSICAL PARAMETERS

Control-surface material	l_a, ft	b_a, ft	m_a, slugs/ft	I_a, slug-ft^2/ft	r_a^2	$\mu_{M=1.6}$
NACA 65A004 wing section[a]						
Steel	0.606	0.0696	0.0145	5.5×10^{-5}	0.782	1,133
Aluminum	.606	.0692	.00593	2.29	.806	469
Magnesium	.606	.070	.00357	1.24	.71	276
Hexagonal wing section[b]						
Magnesium	0.600	0.0679	0.00679	2.39×10^{-5}	0.766	559

[a]The first natural wing frequency for the NACA 65A004 wing section was about 260 cps.

[b]The first natural wing frequency for the 5-percent hexagonal wing section was about 300 cps.

L-816

TABLE 2.- CONTROL-SURFACE DATA

(a) M = 1.3

f_o	f_t	g_o	g_t	k	$\bar{N}_5$	$\bar{N}_6$	$-C_{h_{\dot{\delta}}}$
Hexagonal wing; $\mu r_a^2 = 313$							
68	182	0.0115	0.0023	0.0550	269	0.22	0.024
70	182	.0105	.0022	.0550	267	.19	.021
68	184	.010	.007	.0555	270	1.75	.194
72	183	.0095	.011	.0552	264	2.98	.330
89	188	.0085	.0082	.0568	242	1.97	.224
101	193	.0095	.0092	.0585	228	2.07	.242
101	191	.011	.007	.0578	228	1.25	.144
133	215	.019	.012	.065	193	1.47	.191
133	213	.034	.015	.0645	191	.53	.068
145	222	.013	.012	.0672	180	2.04	.274
146	217	.014	.010	.0658	171	1.16	.153
178	240	.018	.0115	.0725	141	.50	.073
180	242	.014	.0074	.073	140	-.09	-.013
185	245	.0165	.014	.074	135	1.44	.213
65A004 wing; $\mu r_a^2 = 650$							
66	135	0.0085	0.0068	0.0419	495	3.12	0.262
66	136	.0070	.0030	.0422	497	.85	.072
81	142	.0109	.0085	.0440	439	3.25	.286
81	142	.0097	.0075	.0440	439	2.80	.246
81	142	.0091	.0052	.0440	439	1.43	.126
89	146	.010	.0093	.0453	408	3.64	.330
89	147	.0075	.0070	.0457	412	2.80	.256
89	145	.0090	.0050	.045	405	1.04	.094
120	164	.010	.0055	.0508	302	.06	.006
120	165	.010	.0072	.0513	306	1.24	.127
138	175	[a].032	.021	.0544	246	.65	.071
		[b].018	.021			6.50	.706
132	172	[a].018	.027	.0535	267	10.40	1.112
		[b].018	.021			6.50	.695
147	186	.006	.010	.0578	244	4.03	.465
160	192	[a].020	.028	.0595	198	9.10	1.082
		[b].016	.017			3.90	.465
160	190	[a].024	.030	.0589	189	8.50	1.000
		[b].016	.014			1.95	.230

[a]High amplitude.

[b]Lower amplitude.

TABLE 2.- CONTROL-SURFACE DATA - Continued

(b) M = 1.6

f_o	f_t	g_o	g_t	k	$\bar{N}_5$	$\bar{N}_6$	$-C_{h_{\dot{\delta}}}$
Hexagonal wing; $\mu r_a^2 = 427$							
70	160	0.014	0.021	0.0415	345	7.80	0.647
72	163	.011	.020	.0424	344	7.65	.648
71	160	.0107	.023	.0415	343	8.90	.739
90	170	.0114	.021	.0442	307	7.60	.671
90	171	.0103	.0205	.0445	309	7.51	.669
92	170	.0104	.024	.0442	302	8.90	.786
92	170	.010	.0275	.0442	302	10.50	.929
101	172	.0103	.0256	.0446	280	9.40	.838
102	176	.0118	.0259	.0456	284	9.40	.856
148	210	.0097	.0245	.0547	215	8.40	.920
148	201	.010	.024	.0520	196	7.95	.826
146	202	.0115	.023	.0524	204	7.25	.759
147	202	.0078	.0188	.0524	201	6.27	.656
189	233	.0060	.0155	.0606	147	4.95	.600
187	231	.0065	.018	.0606	148	5.85	.710
187	233	.0060	.023	.0606	152	8.15	.989
213	250	.0058	.019	.065	117	6.36	.827
213	251	.0054	.016	.0654	120	5.16	.675
233	265	.0078	.0214	.069	97	6.57	.907
232	260	.0088	.020	.0676	88	5.55	.750

L-816

TABLE 2.- CONTROL-SURFACE DATA - Concluded

(b) M = 1.6

f_o	f_t	g_o	g_t	k	$\bar{N}_5$	$\bar{N}_6$	$-C_{h_\delta}$
65A004 wing; μr_a^2 = 886							
52	111	0.0078	0.016	0.0296	693	12.7	0.752
52	112	.0080	.0154	.0298	696	12.1	.723
53	110	.0073	.0172	.0294	680	13.7	.805
53	113	.0067	.0147	.0301	691	11.7	.705
66	120	.0063	.015	.0321	619	11.6	.745
66	119	.0066	.0164	.0318	614	12.8	.815
65	120	.0085	.0168	.0321	626	12.7	.815
65	120	.0083	.016	.0321	626	12.0	.770
80	130	.0076	.0154	.0347	551	11.1	.770
80	129	.0079	.0164	.0344	545	11.9	.819
80	128	.0060	.0146	.0341	540	10.9	.744
80	129	.0063	.0158	.0344	545	11.9	.819
90	133	.0062	.0165	.0354	480	12.1	.856
90	133	.0063	.0151	.0354	480	10.8	.765
90	133	.0055	.0162	.0354	480	12.1	.856
88	131	.0069	.015	.035	487	10.6	.742
152	176	.0047	.0144	.047	225	9.7	.910
153	176	.0040	.0146	.047	217	10.3	.968
65A004 wing; μr_a^2 = 378							
83	176	0.009	0.026	0.0467	294	9.13	0.852
83	176	.009	.0223	.0467	294	7.72	.711
105	186	.010	.0224	.0493	258	7.26	.717
105	187	.010	.0252	.0495	259	8.33	.825
128	200	.0073	.0215	.0532	223	7.00	.745
128	203	.008	.0213	.0538	228	6.85	.737
144	210	.0085	.0224	.0559	201	6.96	.779
142	210	.008	.021	.0559	206	6.55	.732
142	208	.0078	.0225	.0552	202	7.15	.790
193	240	.0065	.021	.0637	134	6.36	.811
194	240	.0064	.020	.0637	131	5.98	.761
227	260	.0058	.0207	.069	91	6.17	.851
230	259	.0063	.0222	.0685	80	6.50	.890
65A004 wing; μr_a^2 = 196							
144	256	0.0075	0.030	0.0688	134	5.40	0.743
142	256	.0076	.023	.0688	135	4.05	.557
114	242	.0065	.0286	.065	152	5.32	.691
114	246	.0079	.032	.0658	154	5.93	.780

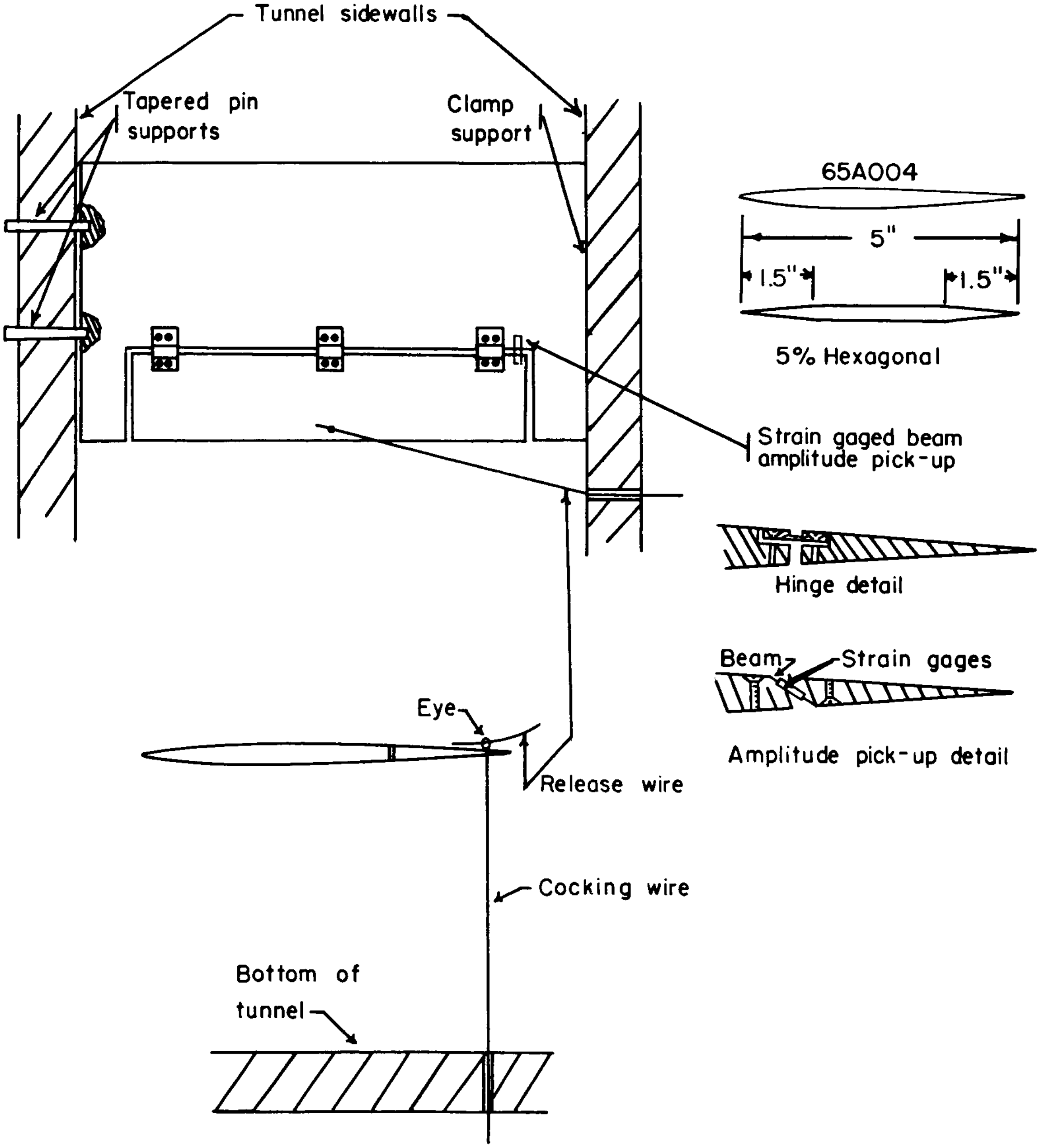

Figure 1.- Sketch of wing and control surface used in tests.

L-816

L-816

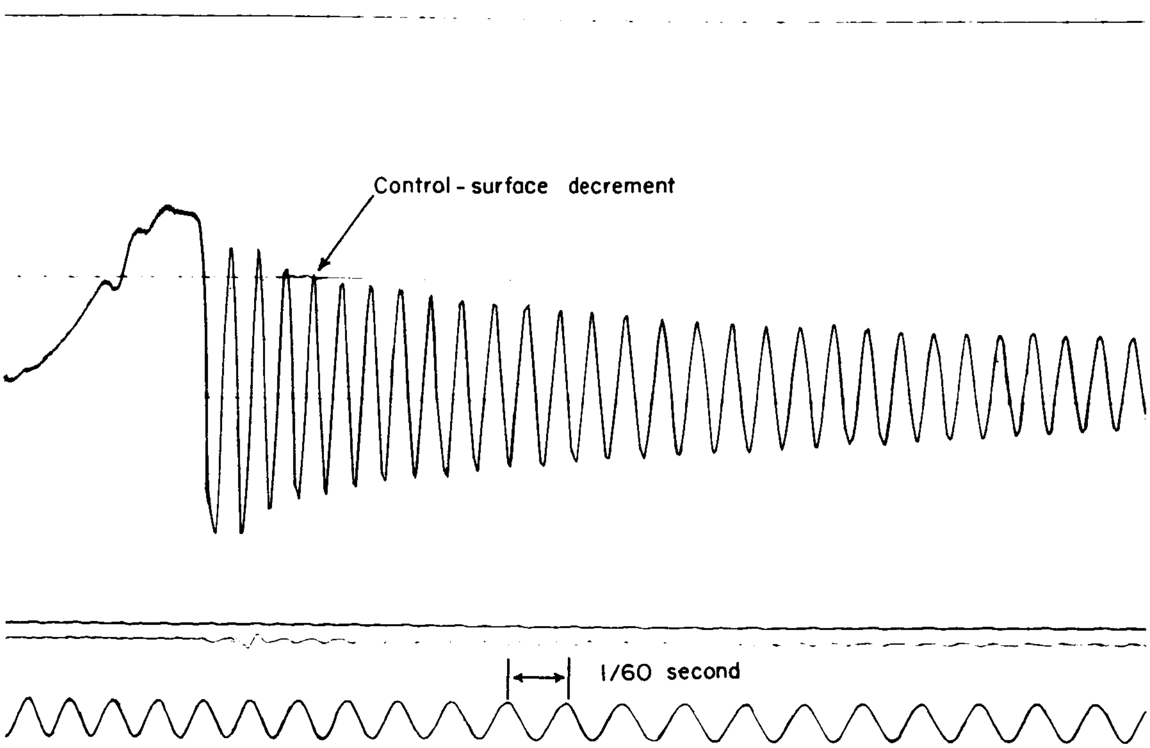

(a) "Wind-off" decrement.

Figure 2.- Sample decrement.

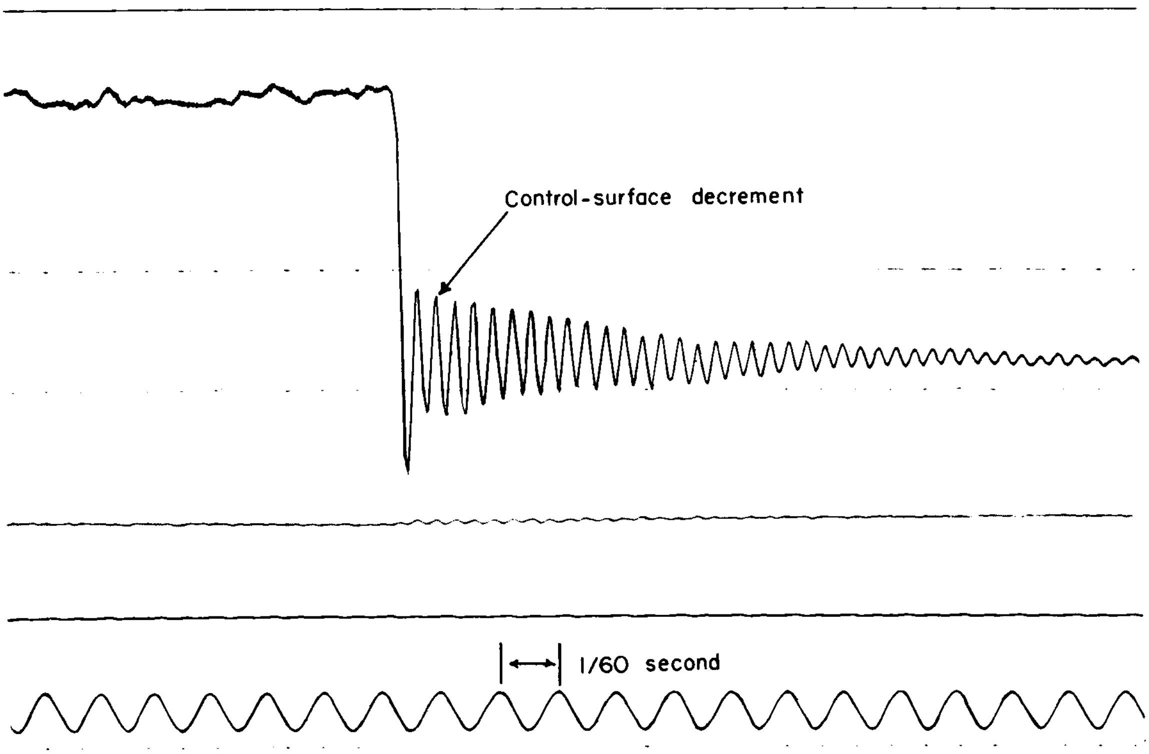

(b) "Wind-on" decrement.

Figure 2.- Concluded.

L-816

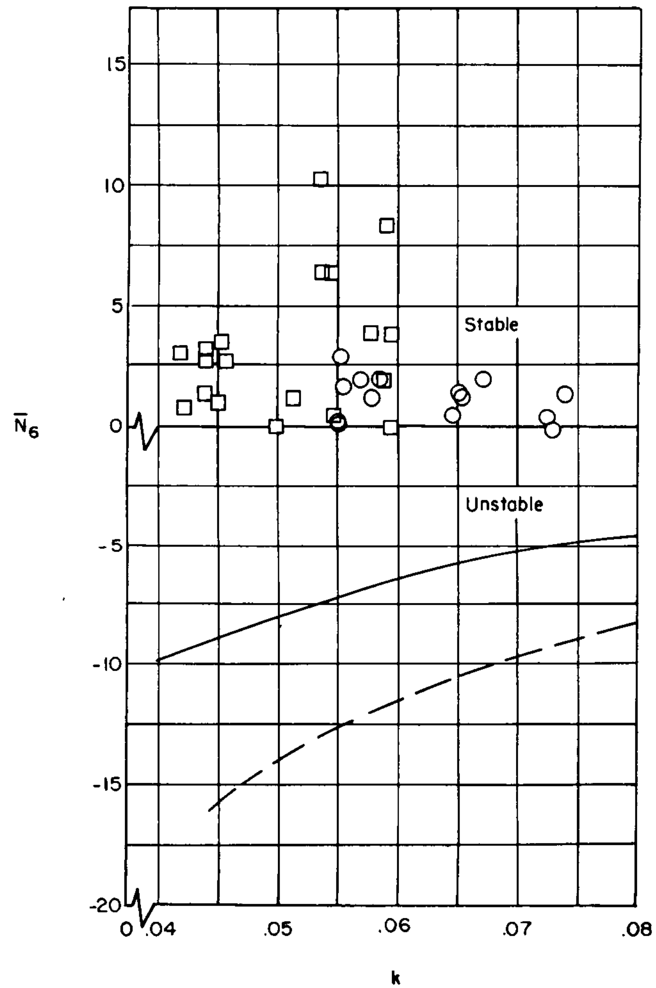

(a) M = 1.3.

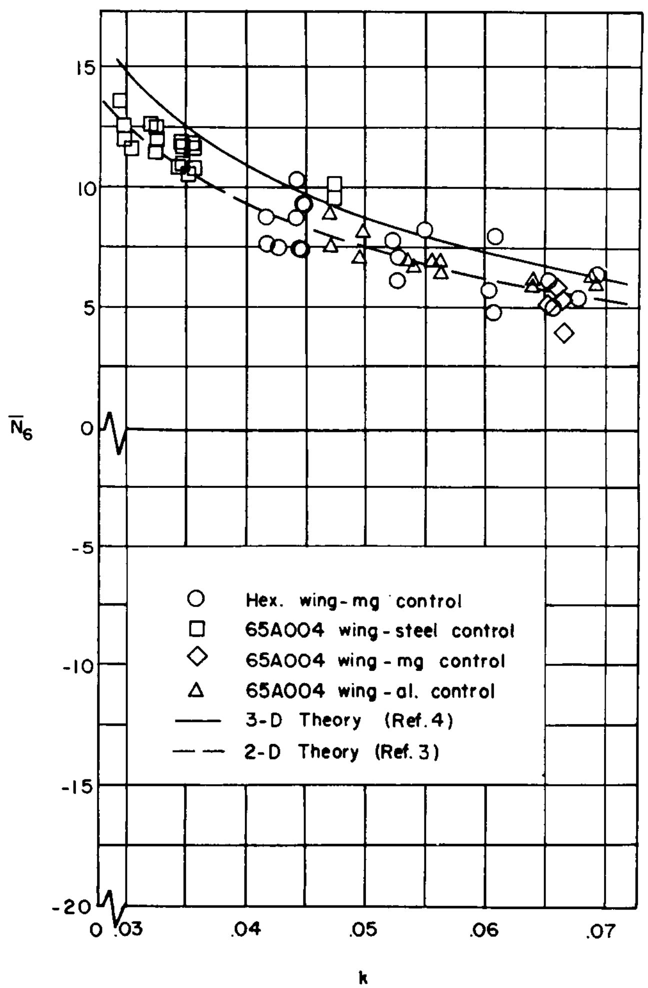

(b) M = 1.6.

Figure 3.- Variation of aerodynamic damping coefficient $\overline{N}_6$ with reduced frequency k at M = 1.3 and 1.6.

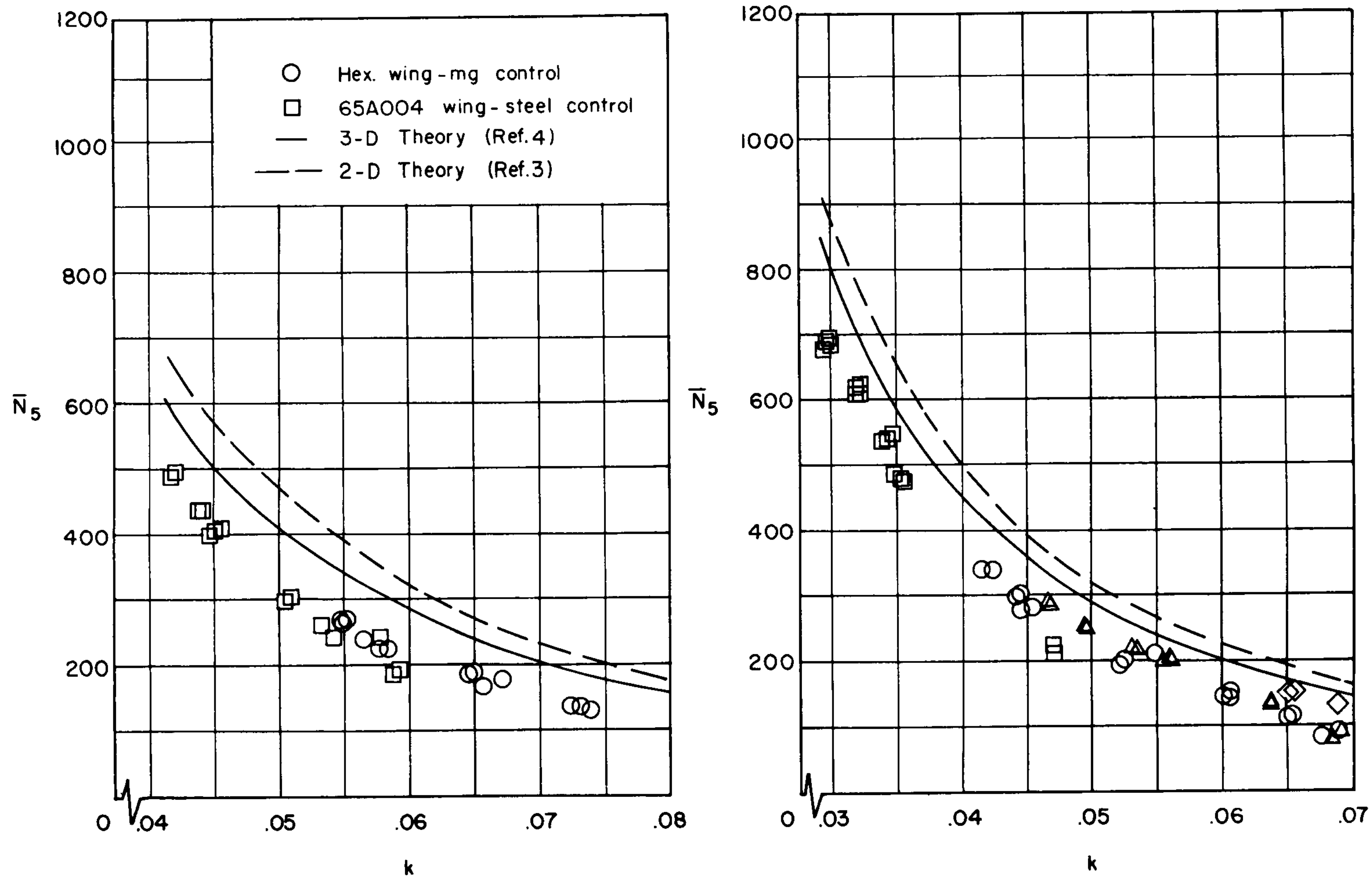

(a) M = 1.3.

(b) M = 1.6.

Figure 4.- Variation of in-phase aerodynamic coefficient $\bar{N}_5$ with reduced frequency k at M = 1.3 and 1.6.

L-816

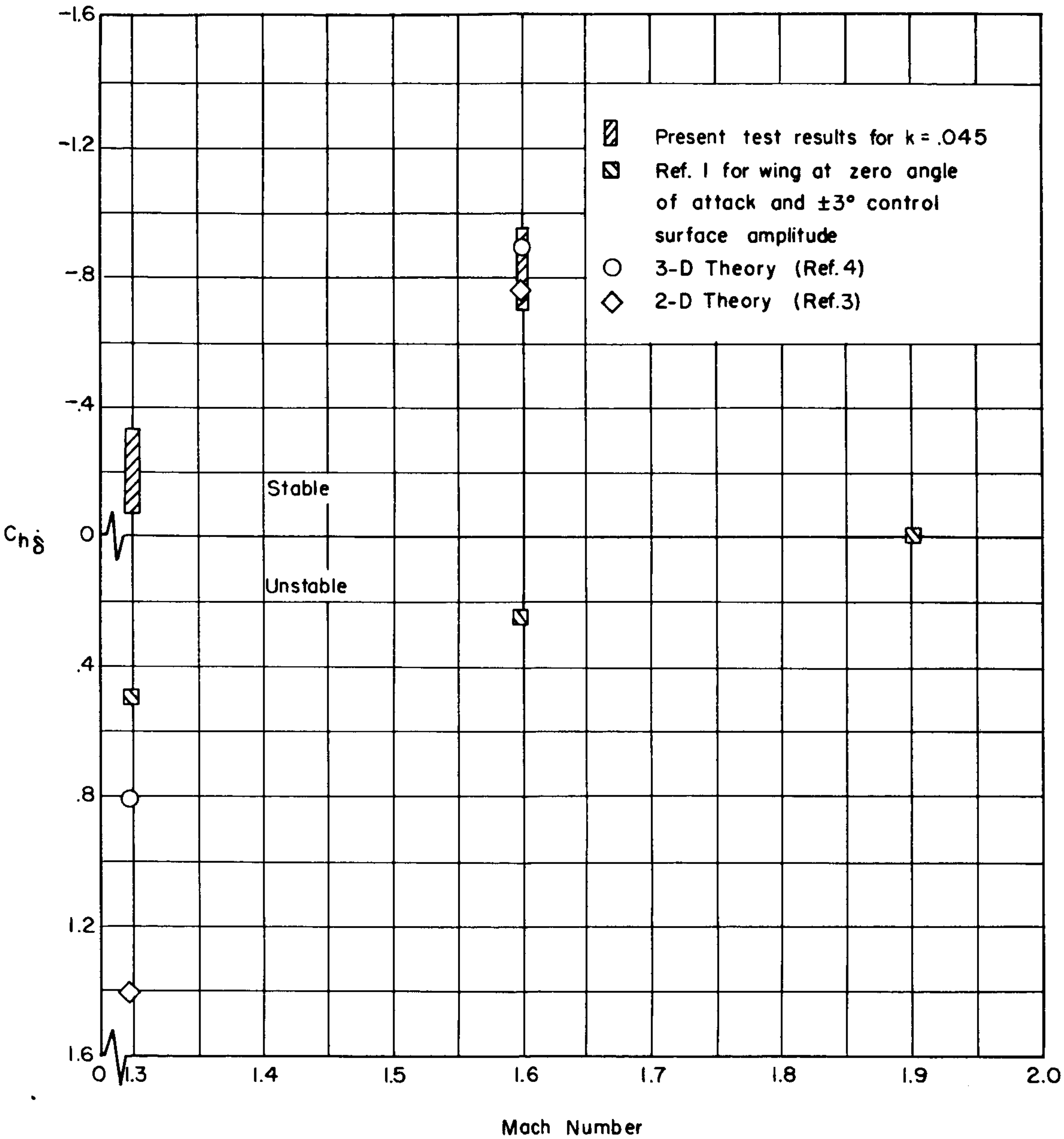

Figure 5.- Variation of damping coefficient $C_{h_{\dot{\delta}}}$ with Mach number and comparison with results of reference 1 at k values of about 0.03.